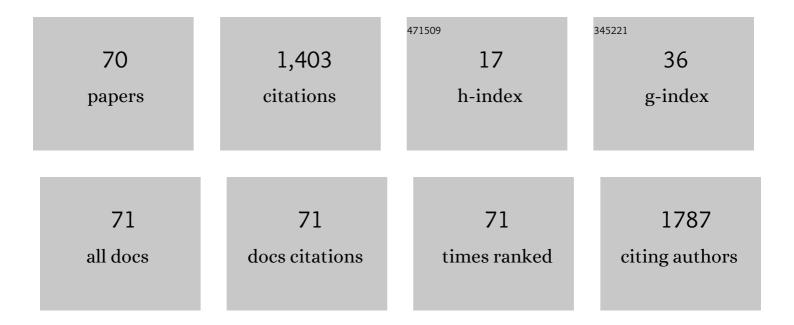
Ping-Ping Chen

List of Publications by Year in descending order

Source: https://exaly.com/author-pdf/6175518/publications.pdf Version: 2024-02-01



DINC-DINC CHEN

#	Article	IF	CITATIONS
1	Single InAs Nanowire Room-Temperature Near-Infrared Photodetectors. ACS Nano, 2014, 8, 3628-3635.	14.6	238
2	High-Responsivity Graphene/InAs Nanowire Heterojunction Near-Infrared Photodetectors with Distinct Photocurrent On/Off Ratios. Small, 2015, 11, 936-942.	10.0	166
3	Visible Light-Assisted High-Performance Mid-Infrared Photodetectors Based on Single InAs Nanowire. Nano Letters, 2016, 16, 6416-6424.	9.1	134
4	Imaging of nonlocal hot-electron energy dissipation via shot noise. Science, 2018, 360, 775-778.	12.6	85
5	High-Polarization-Discriminating Infrared Detection Using a Single Quantum Well Sandwiched in Plasmonic Micro-Cavity. Scientific Reports, 2014, 4, 6332.	3.3	77
6	Distinct Photocurrent Response of Individual GaAs Nanowires Induced by n-Type Doping. ACS Nano, 2012, 6, 6005-6013.	14.6	66
7	Ultrasensitive Mid-wavelength Infrared Photodetection Based on a Single InAs Nanowire. ACS Nano, 2019, 13, 3492-3499.	14.6	45
8	Structure and quality controlled growth of InAs nanowires through catalyst engineering. Nano Research, 2014, 7, 1640-1649.	10.4	37
9	Self-Assembly Growth of In-Rich InGaAs Core–Shell Structured Nanowires with Remarkable Near-Infrared Photoresponsivity. Nano Letters, 2017, 17, 7824-7830.	9.1	37
10	Quality of epitaxial InAs nanowires controlled by catalyst size in molecular beam epitaxy. Applied Physics Letters, 2013, 103, .	3.3	34
11	Orientation Dependence of Electromechanical Characteristics of Defect-free InAs Nanowires. Nano Letters, 2016, 16, 1787-1793.	9.1	30
12	In Situ TEM Observation of Crystal Structure Transformation in InAs Nanowires on Atomic Scale. Nano Letters, 2018, 18, 6597-6603.	9.1	29
13	Quality Control of GaAs Nanowire Structures by Limiting As Flux in Molecular Beam Epitaxy. Journal of Physical Chemistry C, 2015, 119, 20721-20727.	3.1	23
14	Quantum dot single-photon switches of resonant tunneling current for discriminating-photon-number detection. Scientific Reports, 2015, 5, 9389.	3.3	23
15	Au impact on GaAs epitaxial growth on GaAs (111)B substrates in molecular beam epitaxy. Applied Physics Letters, 2013, 102, .	3.3	22
16	Surface-States-Modulated High-Performance InAs Nanowire Phototransistor. Journal of Physical Chemistry Letters, 2020, 11, 6413-6419.	4.6	21
17	Crystal-phase control of GaAs–GaAsSb core–shell/axial nanowire heterostructures by a two-step growth method. Journal of Materials Chemistry C, 2018, 6, 6726-6732.	5.5	20
18	Ultralow Threshold, Single-Mode InGaAs/GaAs Multiquantum Disk Nanowire Lasers. ACS Nano, 2021, 15, 9126-9133.	14.6	19

PING-PING CHEN

#	Article	IF	CITATIONS
19	Photoreflectance and photoreflectance excitation study of optical transitions in GaAsBi/GaAs heterostructure. Journal of Applied Physics, 2018, 123, .	2.5	15
20	Defect-free thin InAs nanowires grown using molecular beam epitaxy. Nanoscale, 2016, 8, 1401-1406.	5.6	14
21	Light-Induced Positive and Negative Photoconductances of InAs Nanowires toward Rewritable Nonvolatile Memory. ACS Applied Electronic Materials, 2019, 1, 1825-1831.	4.3	14
22	High-responsivity and polarization-discriminating terahertz photodetector based on plasmonic resonance. Applied Physics Letters, 2019, 114, .	3.3	13
23	Strongly polarized quantum well infrared photodetector with metallic cavity for narrowband wavelength selective detection. Applied Physics Letters, 2020, 116, .	3.3	13
24	Self-frequency-conversion nanowire lasers. Light: Science and Applications, 2022, 11, 120.	16.6	13
25	Phase purification of GaAs nanowires by prolonging the growth duration in MBE. Journal of Materials Chemistry C, 2017, 5, 5257-5262.	5.5	11
26	Quasiadiabatic electron transport in room temperature nanoelectronic devices induced by hot-phonon bottleneck. Nature Communications, 2021, 12, 4752.	12.8	11
27	Angular dependence of optical modes in metal-insulator-metal coupled quantum well infrared photodetector. AIP Advances, 2016, 6, .	1.3	10
28	Epitaxial GaAs/AlGaAs core–multishell nanowires with enhanced photoluminescence lifetime. Nanoscale, 2019, 11, 6859-6865.	5.6	10
29	High-quality epitaxial wurtzite structured InAs nanosheets grown in MBE. Nanoscale, 2020, 12, 271-276.	5.6	10
30	<i>In situ</i> TEM observation of the vapor–solid–solid growth of <001̄> InAs nanowires. Nanoscale, 2020, 12, 11711-11717.	5.6	9
31	Anomalously Strong Secondâ€Harmonic Generation in GaAs Nanowires via Crystalâ€Structure Engineering. Advanced Functional Materials, 2021, 31, 2104671.	14.9	9
32	High intersubband absorption in long-wave quantum well infrared photodetector based on waveguide resonance. Journal Physics D: Applied Physics, 2018, 51, 225105.	2.8	8
33	Effect of exciton transfer on recombination dynamics in vertically nonuniform GaAsSb epilayers. Applied Physics Letters, 2019, 114, .	3.3	7
34	Band Structure of Wurtzite GaBiAs Nanowires. Nano Letters, 2019, 19, 6454-6460.	9.1	7
35	Characterization of the microstructures and optical properties of CdTe(0Â0Â1) and (1Â1Â1) thin films grown on GaAs(0Â0Â1) substrates by molecular beam epitaxy. Journal of Crystal Growth, 2020, 546, 125756.	1.5	7
36	Enhanced terahertz absorption of quantum wells sandwiched between heavily doped contacts based on micro-cavity resonance. Journal of Applied Physics, 2020, 127, .	2.5	7

PING-PING CHEN

#	Article	IF	CITATIONS
37	Effect of Cd/As flux ratio and annealing process on the transport properties of Cd ₃ As ₂ films grown by molecular beam epitaxy. Materials Research Express, 2020, 7, 106405.	1.6	7
38	Effects of bias and temperature on the intersubband absorption in very long wavelength GaAs/AlGaAs quantum well infrared photodetectors. Journal of Applied Physics, 2014, 115, 124503.	2.5	6
39	Photoluminescence of the single wurtzite GaAs nanowire with different powers and temperatures. Journal of Luminescence, 2014, 152, 258-261.	3.1	6
40	Highly photoresponsive charge-sensitive infrared phototransistors with a dynamically controlled optical gate. Applied Physics Letters, 2016, 109, .	3.3	6
41	Photoconductivity of InN grown by MOVPE: Low temperature and weak light illumination. Applied Physics Letters, 2017, 110, .	3.3	6
42	Free-Standing InAs Nanobelts Driven by Polarity in MBE. ACS Applied Materials & Interfaces, 2019, 11, 44609-44616.	8.0	6
43	Au-catalysed free-standing wurtzite structured InAs nanosheets grown by molecular beam epitaxy. Nano Research, 2019, 12, 2718-2722.	10.4	6
44	Bi2Te3 photoconductive detector under weak light. Journal of Applied Physics, 2019, 126, .	2.5	6
45	Cut-off wavelength manipulation of pixel-level plasmonic microcavity for long wavelength infrared detection. Applied Physics Letters, 2019, 114, .	3.3	6
46	Anomalous Photoelectrical Properties through Strain Engineering Based on a Single Bent InAsSb Nanowire. ACS Applied Materials & Interfaces, 2021, 13, 5691-5698.	8.0	6
47	Pressureâ€Induced Superconductivity in HgTe Singleâ€Crystal Film. Advanced Science, 2022, 9, e2200590.	11.2	6
48	In-situ PR study of the confined states in AlGaAs/GaAs surface QW. Journal of Crystal Growth, 2001, 227-228, 108-111.	1.5	5
49	Far infrared reflection spectra of InAsxSb1â^x (x = 0-0.4) thin films. Journal of Applied Physics, 2013, 113 213112.	, 2.5	5
50	High efficiency optical coupling in long wavelength quantum cascade infrared detector via quasi-one-dimensional grating plasmonic micro-cavity. Journal of Applied Physics, 2017, 121, .	2.5	5
51	Raman mapping of laser-induced changes and ablation of InAs nanowires. Applied Physics A: Materials Science and Processing, 2014, 115, 885-893.	2.3	4
52	Formation of GaAs/GaSb Core-Shell Heterostructured Nanowires Grown by Molecular-Beam Epitaxy. Crystals, 2017, 7, 94.	2.2	4
53	Evolution of morphology and microstructure of GaAs/GaSb nanowire heterostructures. Nanoscale Research Letters, 2015, 10, 108.	5.7	3
54	InN superconducting phase transition. Scientific Reports, 2019, 9, 12309.	3.3	3

PING-PING CHEN

#	Article	IF	CITATIONS
55	Linear array of charge sensitive infrared phototransistors for long wavelength infrared detection. Applied Physics Letters, 2020, 116, 233501.	3.3	3
56	Photoelectronic Properties of End-bonded InAsSb Nanowire Array Detector under Weak Light. Nanoscale Research Letters, 2021, 16, 13.	5.7	3
57	Anisotropic Hot-Electron Kinetics Revealed by Terahertz Fluctuation. ACS Photonics, 2021, 8, 2674-2682.	6.6	3
58	Photodetectors: High-Responsivity Graphene/InAs Nanowire Heterojunction Near-Infrared Photodetectors with Distinct Photocurrent On/Off Ratios (Small 8/2015). Small, 2015, 11, 890-890.	10.0	2
59	Dual-color charge-sensitive infrared phototransistors with dynamic optical gate. Applied Physics Letters, 2021, 119, 103505.	3.3	1
60	Independent Control of Mode Selection and Power Extraction in Terahertz Semiconductor Lasers. ACS Photonics, 2022, 9, 1973-1983.	6.6	1
61	Effect of V/III ratio on the structural quality of InAs nanowires. , 2014, , .		0
62	Cavity modes in hybrid structure of QWIP and plasmonic cavity. , 2014, , .		0
63	Room-temperature, high-gain, broad-spectrum InAs nanowire infrared photodetectors. , 2015, , .		0
64	Scanning THz Noise Microscopy of Operating Nano-devices. , 2018, , .		0
65	Two-Dimensional Energy Band Engineering in GaAs/AlGaAs Core–Shell Nanowires by Crystal-Phase Switching for Charge Manipulation. ACS Applied Nano Materials, 2019, 2, 3323-3328.	5.0	0
66	The temperature dependence of anomalous magnetoresistance and weak antilocalization in HgTe/CdTe (111) quantum wells. Journal of Applied Physics, 2020, 127, 075108.	2.5	0
67	Axiotaxy driven growth of belt-shaped InAs nanowires in molecular beam epitaxy. Nano Research, 2021, 14, 2330.	10.4	0
68	Metallic cavity quantum well infrared photodetector for filter-free SF6 gas imaging. Optical and Quantum Electronics, 2021, 53, 1.	3.3	0
69	Modulation and optimization of terahertz absorption in micro-cavity quantum well structures by graphene grating. Journal Physics D: Applied Physics, 2022, 55, 165104.	2.8	0
70	Multiple Modes Response of Coâ€Aperture 2D/1D Phototransistors. Advanced Materials Interfaces, 0, , 2102568.	3.7	0